Drug Design, Development and Therapy

Dovepress

open access to scientific and medical research

Open Access Full Text Article

ORIGINAL RESEARCH

Orally Deliverable Dual-Targeted Pellets for the Synergistic Treatment of Ulcerative Colitis

Xiaomeng Tang[1–3,*]
Meng Yang[4,*]
Yongwei Gu[1,2]
Liangdi Jiang[1,2,5]
Yue Du[1,2,5]
Jiyong Liu[1–3]

[1]Department of Pharmacy, Fudan University Shanghai Cancer Center, Fudan University, Shanghai, 200032, People's Republic of China; [2]Department of Oncology, Shanghai Medical College, Fudan University, Shanghai, 200032, People's Republic of China; [3]Department of Pharmacy, Changhai Hospital, Naval Medical University, Shanghai, 200433, People's Republic of China; [4]Department of Pharmacy, Shanghai Ninth People Hospital, Shanghai Jiao Tong University, Shanghai, 200011, People's Republic of China; [5]College of Pharmacy, Shandong University of Traditional Chinese Medicine, Jinan, Shandong, 250355, People's Republic of China

*These authors contributed equally to this work

Purpose: The effective treatment of ulcerative colitis (UC) poses substantial challenges, and the aetiopathogenesis of UC is closely related to infectious, immunological and environmental factors. Currently, there is a considerable need for the development of orally bioavailable dosage forms that enable the effective delivery of therapeutic drugs to local diseased lesions in the gastrointestinal tract.

Methods: Berberine (BBR) and *Atractylodes macrocephala* Koidz (AM) volatile oil, derived from the Chinese herbs *Coptis chinensis* Franch and *Atractylodes macrocephala* Koidz, have anti-inflammatory and immunomodulatory activities. In this study, we prepared colon-targeted pellets loaded with BBR and stomach-targeted pellets loaded with AM volatile oil for the synergistic treatment of UC. The Box–Behnken design and β-cyclodextrin inclusion technique were used to optimize the enteric coating formula and prepare volatile oil inclusion compounds.

Results: The two types of pellets were spherical and had satisfactory physical properties. The pharmacokinetic results showed that the AUC and MRT values of the dual-targeted (DPs) pellets were higher than those of the control pellets. In addition, in vivo animal imaging confirmed that the DPs could effectively deliver BBR to the colon. Moreover, compared with sulfasalazine and monotherapy, DPs exerted a more significant anti-inflammatory effect by inhibiting the expression of inflammatory factors including IL-1β, IL-4, IL-6, TNF-α and MPO both in serum and tissues and enhancing immunity by decreasing the production of IgA and IgG.

Conclusion: The DPs play a synergistic anti-UC effect by exerting systemic and local anti-inflammatory and provide an effective oral targeted preparation for the treatment of UC.

Keywords: ulcerative colitis, oral dual-targeted pellets, synergistic treatment, berberine, AM volatile oil

Introduction

Ulcerative colitis (UC), known as chronic nonspecific ulcerative colitis, is a chronic and debilitating inflammatory disease that results from a complex interplay between infectious, immunological, environmental and microbial factors.[1] The main clinical manifestations of UC are digestive system symptoms and difficulty healing, for as long as several months to decades.[2,3] Depending on the duration and extent of inflammation, long-standing UC patients (~18%) have a much higher risk of developing colitis-associated colorectal cancer (CAC).[4–6] At present, adrenal corticosteroids (prednisone) and aminosalicylic acid (mesalazine) are commonly used drugs for the treatment of UC, but these drugs can only relieve symptoms and often have many side effects. In addition, the

Correspondence: Jiyong Liu
Department of Pharmacy, Fudan University Shanghai Cancer Center, Fudan University, Shanghai, 200032, People's Republic of China
Tel/Fax +86-21-64175590
Email liujiyong@fudan.edu.cn

Received: 31 May 2021
Accepted: 23 August 2021
Published: 29 September 2021

Graphical Abstract

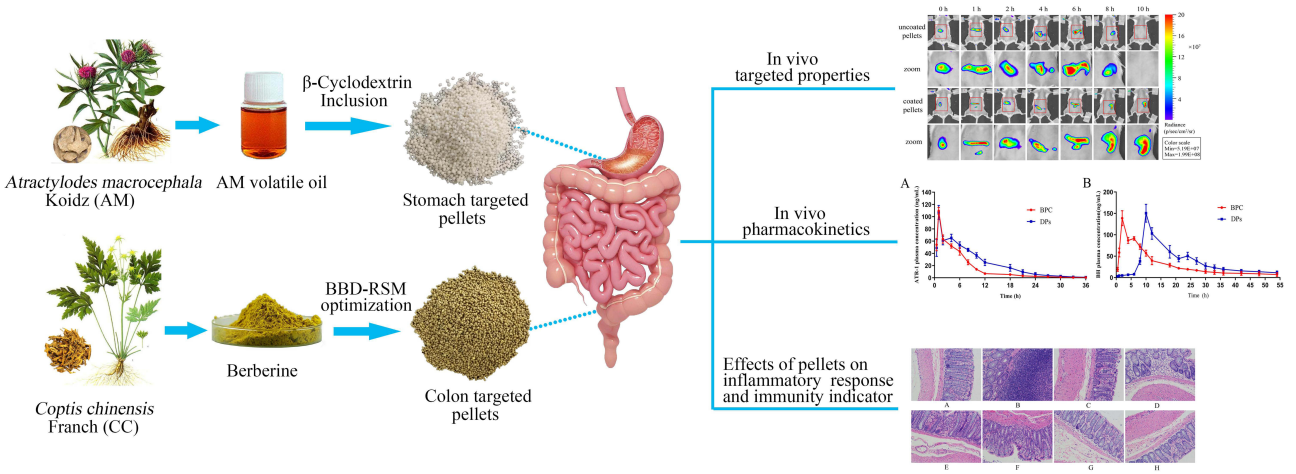

effectiveness and safety of other reported drugs, such as immunosuppressive agents (azathioprine), vary greatly among different individuals.[7] Therefore, there is a considerable need to develop expedient and practical formulations that can effectively treat UC.

Atractylodes macrocephala Koidz (AM) has long been used to treat gastrointestinal hypofunction.[8] Volatile oil contains volatile components extracted from AM and can improve gastrointestinal function, enhance body immunity and exert anti-inflammatory effects.[9] However, the components of AM volatile oil are less stable and can easily decompose and deteriorate under the action of oxygen, light and heat. As reported, the technique of cyclodextrin inclusion can prevent oxidation and decomposition of the volatile oil and simultaneously make the liquid drug a powder, which can improve the drug stability during the preparation and storage processes.[10] Further pelleting of the inclusion complex can facilitate patient administration and mask undesirable odours of the volatile oil.

Berberine (BBR) is the active ingredient of *Coptis chinensis* Franch (CC) and can reduce the symptoms of colitis, attenuate mucosal barrier damage,[11] and restore barrier function.[12] However, BBR is a BCS class II compound that exhibits low bioavailability when orally administered and is mainly well absorbed in the intestine.[13] Therefore, it is necessary to improve the solubility and bioavailability of BBR and to facilitate targeted delivery of BBR to diseased colon tissues to enhance the local anti-inflammatory effect.

Dosage forms play an important role in the absorption and transport of oral preparations. However, clinical treatments for UC are always absorbed or degraded before reaching the colon, leading to less accumulation in ulcer lesions and affecting efficacy. The oral colon-targeted drug delivery system (OCDDS) uses appropriate preparation technology to prevent the drug from being released in the stomach, duodenum, jejunum and front end of the ileum after oral administration.[14,15] Thus, it can deliver drugs to the lesion and exert a local or systemic therapeutic effect.[16] There are various types of oral colon-targeted drug delivery systems, including pH type, enzymatic contact type, time-dependent type, pressure control type, bioadhesive type, prodrug type, combination type, etc.[17,18] At present, the varieties that have been on the market or entered clinical research are mostly coated with pH-dependent materials. In addition, pellets are a multiunit drug delivery system that can increase the contact area between the drug and gastrointestinal tract, promoting absorption and bioavailability.[19] Therefore, the development of oral colon-targeted pellets may improve BBR oral bioavailability and colon targeting.

Currently, commercially available OCDDS are mostly of the pH-sensitive coating type based on the pH of the gastrointestinal tract (stomach 0.9–1.5, small intestine 6.5–7, colon 6.8–7.5).[20] Directly marketed polymer materials, such as EUDRAGIT®L 30D-55 and EUDRAGIT®FS 30D, with intrinsic pH-sensitive properties, are not suitable for targeted drug delivery to the colon.[21] Therefore, we optimized mixed polymer materials to allow the coated

preparation to release a large amount of the drug after reaching the colon.

In this study, BBR and AM volatile oils were loaded into colon-targeted pellets and stomach-targeted pellets, respectively, to prepare DPs for synergistic treatment of UC. After administration, BBR was released in the colon to exert a local targeting anti-inflammatory effect, while AM volatile oil was absorbed in the stomach to exert a systemic immunoregulatory effect. In this study, we optimized the pellet preparation process, characterized the pellet physicochemical properties and evaluated colonic targeting. In addition, the pharmacokinetic characteristics of DPs in rats were detected. A DSS-induced rat UC model was constructed to investigate the pharmacodynamic properties of the developed DPs. These results could substantially contribute to UC management and might provide a pharmaceutical strategy for the treatment of gastrointestinal diseases.

Materials and Methods

Materials

Atractylodes macrocephala Koidz volatile oil and *Coptis chinensis* Franch extract were purchased from Xi'an Xiaocao Plant Technology Co., Ltd. (Xi'an, Shanxi, China). Atractylenolide I (AT-1) and berberine hydrochloride standards were purchased from the National Institute for Food and Drug Control (Beijing, China). β-Cyclodextrin (β-CD) was purchased from Tianli Pharmaceutical Excipients Co., Ltd. (Qufu, Shandong, China). Microcrystalline cellulose (MCC) was purchased from Huzhou Linghu Xinwang Chemical Co., Ltd. (Huzhou, Zhejiang, China). Lactose was purchased from DMV-Fonterra Excipients GmbH & Co. KG (Goch, Germany). Crosslinking polyvinylpyrrolidone XL was purchased from Shanghai Yuanye Biological Technology Co., Ltd. (Shanghai, China). Tween 80 was purchased from Shanghai Lingfeng Chemical Reagent Co., Ltd. (Shanghai, China). EUDRAGIT® FS 30 D and EUDRAGIT® L 30D-55 were kindly donated by Evonik Röhm GmbH. (Darmstadt, Germany). Hypromellose (HPMC), triethylcitrate (TEC) and sulfasalazine (SASP) were purchased from Aladdin Reagent Co., Ltd. (Shanghai, China). Glycerine monostearate (GMS) was purchased from Alfa Aesar Chemical Co., Ltd. (Ward Hill, US). Dextran sulfate sodium salt (DSS, MV: 36000~5000) was purchased from Shanghai Yisheng Biological Technology Co., Ltd. (Shanghai, China). Sulfo CY7 NHS ester was purchased from Xi'an Ruixi Biological Technology Co., Ltd. (Xi'an, Shanxi, China). HPLC-grade acetonitrile and methanol were purchased from Tedia Co., Ltd. (Shanghai, China). The other chemicals and solvents used in the study were of analytical reagent grade.

Animals

Sprague-Dawley (SD) rats (male, 180 ± 20 g, Experimental Animal Center of Naval Medical University, Shanghai, China; certificate no. SCXK (Hu) 2017–0002) and BALC/c mice (male, 18 ± 2 g) were utilized for all the in vivo studies. The rats were acclimatized for at least 7 days. Animal experiments were performed according to the protocols evaluated by the ethics committee of the Second Military Medical University (Shanghai, China) and conformed to the National Institutes of Health Guide for the Care and Use of Laboratory Animals.

Preparation of β-CD Inclusion Complex and Pellet Cores

The AM volatile oil/β-CD inclusion complex was first prepared to improve oxidative deterioration while masking the taste. At the same time, the solidification of the liquid drug also laid a foundation for the subsequent preparation of gastric coated pellets. The resulting product was analysed using differential scanning calorimetry (DSC) and X-ray powder diffraction (XRD) to confirm whether the inclusion was successful. The GPs and EPs cores were prepared using the extrusion-spheronization method. EPs cores coated with 4% HPMC as a sub coating layer (Sub-Ps) were also prepared for further coating. The enteric coating dispersion was prepared by mixing EUDRAGIT®FS 30D, EUDRAGIT® L 30D-55, GMS, TEC, Tween-80 and purified water. The coating process parameters are summarized in Table S1. For a more detailed description of the preparation process and characterization parameters, see the Supplementary Material-Methods.

BBD-RSM-Based Enteric Coating Optimization

Polymer ratio, plasticizer concentration and coating weight gain are the three key factors that regulate the release rate of film-controlled pellets. Therefore, the range of values of each factor was determined by single-factor experiments in a previous study. Thereafter, a Box-Behnken design (BBD)

with a three-factor ratio of EUDRAGIT®FS 30D to EUDRAGIT®L 30D-55 (g/g, X_1), plasticizer concentration (%, X_2) and coating weight gain (%, X_3) was used to optimize the enteric coating formula. This technology is suitable for the investigation of quadratic response surfaces, thus enabling optimization of a process with a small number of experimental runs. The design consists of replicated centre points and a set of points lying at the midpoint of each edge of the multidimensional cube that defines the area of interest.[19]

Response surface modelling (RSM) was performed with Design Expert 8.0 (StateEase Inc., Minneapolis, MN). Table 1 summarizes the factors and levels of independent variables. The chosen dependent variables were the cumulative release percentage values of BBR dissolved in a determined time (after 2, 6 and 12 h).

Characterization of Pellets

Morphological Characterization

Pellet size was represented by the average of the length and breadth values determined using a digital Vernier calliper (Shanghai Meinaite Industry Co., Ltd. Shanghai, China). For each pellet type, 20 pellets were randomly characterized, and an average result was calculated.[22] The pellet size distribution of GPs and EPs was determined by the sieving method with diameters of 550–880 μm (30–18 mesh) or 830–1400 μm (20–12 mesh). The results are shown as the percentage of each size fraction. Pellets coated with a thin gold layer were examined via scanning electron microscopy (SEM; HITACHI-S3400N, Japan) to analyse shape and surface morphology.[23]

Roundness, Friability and Bulk Density

Plane-critical stability (PCS) was used to reflect the roundness of the pellets. During the measurement, 20 g of the pellets were laid flat on a glass plate, and one end of the glass plate was slowly lifted. The critical angle (θ) of the plane formed by the inclined plane and the horizontal plane before the pellets start to roll is measured. The smaller the value of θ is, the better the roundness of the pellets.[19]

Pellet friability (*Fr*) was determined using a multipurpose tablet tester (78X-3C, Shanghai Huanghai Drug Testing Instrument Co., Ltd. Shanghai, China). Approximately 50 g of the two pellet types was weighed and added to an abrasion drum together with 200 glass beads (2 mm in diameter). The abrasion drum was rotated at 25 r/min for 10 min. The content of the abrasion drum was sieved using a 550 μm (30 mesh) or 830 μm (20 mesh) sieve, and the fraction below 550 μm or 830 μm was weighed. Friability was measured in triplicate and calculated as follows.[19]

$$Fr(\%) = \frac{Fraction\ <550\mu m(\mathrm{g})}{Total\ sample} \times 100\ (\mathrm{GPs})$$

$$Fr(\%) = \frac{Fraction\ <830\mu m(\mathrm{g})}{Total\ sample} \times 100\ (\mathrm{EPs})$$

Bulk density was measured with 50 g of pellets, which were (*M*) weighed, placed in a 100 mL graduated glass cylinder and then dropped from 5 cm away from the table.[24] The occupied volume (*V*) by the pellets was read precisely, and the bulk density (d) was obtained with the formula d = *M*/*V*. Three batches of pellets were measured in parallel.

Drug Loading Analysis Using HPLC and HPLC-QQQ-MS

Drug loading was defined as the percentage of drug embedded in a unit weight of pellets. Fifty milligrams of pellets were ground and dissolved in 50 mL of methanol. Then, the mixture was ultrasonicated and filtered through a 0.45 μm membrane filter. The samples were store at 4 °C for testing.[25]

For EPs, the BBR concentration was analysed using HPLC (Agilent 1200 series, USA). The mobile phase was composed of acetonitrile and water with 0.05 mol/L potassium dihydrogen phosphate (adjusted with phosphoric acid to pH=3, 30/70, v/v). The flow rate and wavelength were set at 1 mL/min and 345 nm, respectively. For GPs, AT-1 (the active ingredient in AM volatile oil) was

Table 1 Factors and Their Levels in the Box-Behnken Design and Responses

Factors	Levels			Responses
	−1	0	1	
Ratio of EUDRAGIT®FS 30D to EUDRAGIT®L 30D-55 (g/g, X_1)	1:2	1.25:1	2:1	Cumulative drug release in 2 h (%, Y_1)
Plasticizer concentration (%, X_2)	5	10	15	Cumulative drug release in 6 h (%, Y_2)
Coating weight gain (%, X_3)	10	15	20	Cumulative drug release in 12 h (%, Y_3)

quantitatively analysed using HPLC-QQQ-MS (Agilent Technologies Inc., USA). The mobile phase was composed of methanol and water with 0.1% (v/v) acetic acid (75/25, v/v). The other parameters were as follows: column temperature, 35 °C; flow rate, 0.3 mL/min; dry gas (N_2) temperature, 350 °C; nebulizer gas (N_2) pressure, 20 psi; fragmentor voltage, 165 eV; collision energy, 35 eV; positive ion monitoring mode; and m/z = 231.1→128.1.

In vitro Drug Release Study

The pH dissolution method was used to evaluate drug release from pellets.[26] The GPs quickly disintegrated completely in the artificial gastric juice, resulting in a high release rate (pH 1.2, cumulative release over 98% in 5 min). The release of BBR from EPs was determined by using a ChP (2020 edition) dissolution apparatus II (basket method) at a rotation speed of 100 r/min in 750 mL of dissolution medium at 37 ± 0.5 °C under sink conditions. The dissolution test was performed as follows: pH 1.2 for 2 h followed by phosphate buffer at pH 6.8 for 4 h and phosphate buffer at pH 7.6 for 18 h.[27] The concentration of BBR in different samples was measured via HPLC after filtration (0.45 μm). The dissolution test for Sub-Ps and EPs was carried out six times.

In vivo Imaging-Based Colon-Targeted Study of EPs

To investigate the transport and release characteristics of EPs in the mouse gastrointestinal tract, the mice were administered fluorescein-containing EPs (during the preparation of the pellet core, CY7 aqueous solution was used instead of water as a wetting agent) or uncoated pellet cores. Then, the mice were anaesthetized with isoflurane and fixed in an imaging apparatus (Quick View 3000, Bio-Real Sciences Technology Co., Ltd. Austria) at predetermined time points (0 h, 1 h, 2 h, 4 h, 6 h, 8 h, 10 h) after administration. The excitation light wavelength was set to 655 nm, the emission light wavelength was 716 nm, and the exposure time was 3 s.[28]

In vivo Pharmacokinetics Study

The rats were fasted for 12 h with free access to water and were randomly sorted into two groups, with three rats in each group. The two groups were given DPs or bulk pharmaceutical chemicals (BPC, a mixture of BBR and AM volatile oil) by means of oral administration at doses of 200 mg/kg BBR and 50 mg/kg AT-1. Blood samples were collected from the rats via the eye retro-orbital vein at specific intervals of 0, 0.5, 1, 2, 4, 6, 8, 10, 12, 18, 21, 24, 27, 30, 33, 36, 42, 48 and 54 h. The blood samples were immediately subjected to centrifugation (Eppendorf (China), Ltd. Shanghai, China) at 3000 rpm for 15 min. The supernatant was then kept in a freezer at −20 °C for further analysis. Before analysis, plasma samples were protein precipitated with methanol and acetonitrile and dried with nitrogen at 40 °C. The sample was reconstituted in 100 μL methanol and centrifuged before HPLC-QQQ-MS analysis.

Standard methods were used to calculate the pharmacokinetic parameters AUC, half-life ($t_{1/2}$) and MRT using Kinetica 5.0 software (Thermo Fisher Scientific Inc. Waltham, MA, USA). C_{max} and T_{max} were directly computed from the plasma concentration versus time plot. Furthermore, the relative bioavailability (F_{rel}) with reference to the AUC of the developed DPs group compared to the BPC group was calculated using the equation given below.[29]

$$F_{rel}\frac{AUC^{A}}{AUC^{B}} \times 100\%$$

where F_{rel} is the relative bioavailability and AUC^{A} and AUC^{B} are the areas under the drug concentration-time curves of DPs (test) and BPC (reference), respectively.

The concentrations of BBR and AT-1 in plasma were also determined using HPLC-QQQ-MS. The mobile phase was composed of acetonitrile (phase A) and water with 0.1% (v/v) acetic acid (phase B). For BBR, m/z =336.2→320.2, and the operating parameters were set as follows: nebulizer gas (N_2), 20 psi; fragmentor voltage, 155 eV; collision energy, 30 eV; and drying gas (N_2) temperature, 320 °C. For AT-1, the mobile phase ratio was A:B=75:25, and the remaining parameters were the same as before.

Anti-Ulcerative Colitis Analysis

Induction of a UC Rat Model and Experimental Design

UC was induced by replacing the rats' drinking water with a 5% (w/v) DSS solution for 7 days according to a previously described procedure.[30] Eighty rats were randomly divided into eight groups: Group A (normal control group) received tap water for 14 days; Group B (model control group) received DSS (5% w/v) in drinking water for 6 days, after which the animals received regular tap water for 7 days; and Group C received DSS (5% w/v)

water for 6 days followed by treatment with sulfasalazine (SASP suspended in 0.5% w/v normal saline, 100 mg/kg). Groups D-H received DSS (5% w/v) similar to group C. Group D received GPs (equivalent to 50 mg/kg AT-1), group E received EPs (equivalent to 200 mg/kg BBR) for 7 days after DSS administration, and group F-H received DPs (equivalent to 50 mg/kg AT-1 and 50, 100, 200 mg/kg BBR) for 7 days after DSS administration. The rats were treated once per day P.O. for 7 days (groups A and B received normal saline instead of treatment drug), and their body weight was recorded daily. The beginning of the UC model induction was considered day 1. Rat body weight was recorded daily. Blood samples collected from the rats via the eye retro-orbital vein were used to determine IL-1β, IL-4, IL-6, TNF-α, MPO, IgA and IgG concentrations. The rats were sacrificed by cervical dislocation on day 14. The colon length was measured from the ileocaecal junction to the anal verge. After that, the colon tissues were collected for scoring, gross morphology, histopathological analysis and determination of the expression levels of various inflammatory factors. In addition, the spleen and thymus were isolated to calculate the spleen and thymus index.

Colon/Body Weight Ratio

The dissected colon tissues were opened longitudinally along the mesenteric edge and washed with ice-cold physiological saline to remove luminal content before weighing. The colon/body weight ratio (C/B ratio) was an index used to quantify the inflammation and was calculated as a quotient of the 10-cm colon wet weight compared with the total body weight of each rat.[31]

Evaluation of Clinical Colitis Activity

The clinical activity of colitis, including weight loss, stool consistency and rectal bleeding, was evaluated to confirm the disease activity index (DAI). The DAI was determined by calculating the average of the above three parameters on a scale of 0–4 based on the criteria shown in Table S3.[32–34]

Assessment of Macroscopic Injury

For assessment of macroscopic injury, the whole distal colon was examined by an independent observer who was unaware of the research groups. The criteria and scale employed to grade macroscopic injury are described in Table S4.[35,36]

Histological Evaluation

A histological scoring system was used to evaluate microscopic colonic changes. Colon tissue samples of 1 cm cut from the distal colon were prepared as a "Swiss roll" for full-length histopathology evaluation. The "Swiss roll" of each group was immersed in 10% neutral formaldehyde and subsequently embedded in paraffin. Sections of 5 μm thickness were stained with haematoxylin and eosin (H&E) to assess the degree of inflammation. The slides were then examined in a blinded fashion by a pathologist based on a scale that graded the presence of oedema, erosion-ulceration, crypt damage and inflammatory area percentage using a standard light microscope as described previously. The basis of inflammation scoring based on assessment of microscopic (100×) histological changes is shown in Table S5.[37,38]

Determination of IL-1β, IL-4, IL-6, TNF-α, IgA, and IgG Levels and MPO Activity

Cytokines are considered crucial signals in the intestinal immune system, and immune cells, such as T cells, dendritic cells, macrophages, and intestinal epithelial cells, are involved in the secretion of various cytokines that regulate the inflammatory response in UC.[39] Thus, the levels of IL-1β (Multi Sciences Rat IL-1β ELISA Kit, Hangzhou, China), IL-4 (Multi Sciences Rat IL-4 ELISA Kit, Hangzhou, China), IL-6 (Multi Sciences Rat IL-6 ELISA Kit, Hangzhou, China) and TNF-α (Thermo Fisher Rat TNF-α ELISA Kit, Vienna, Austria) in the serum and colon tissue samples were determined according to the manufacturer's instructions using the appropriate ELISA Kits. MPO (Cusabio Rat MPO ELISA Kit, Wuhan, China), IgA (Multi Sciences Rat IgA ELISA Kit, Hangzhou, China) and IgG (Multi Sciences Rat IgG ELISA Kit, Hangzhou, China) levels in the serum samples were also measured using commercially available ELISA kits according to the manufacturers' instructions. One unit of MPO activity was defined as the quantity of enzyme able to convert 1 μmol of hydrogen peroxide to water in 1 min at room temperature. The results are expressed in U/g of tissue.

Statistical Analysis

All data are expressed as the mean ± SD, and statistical analysis was performed with SPSS 20.0 statistical software. Comparisons between groups of parametric data were made using one-way analysis of variance (ANOVA) followed by Bonferroni's test. Nonparametric statistical analysis was performed with a Kruskal–Wallis test

followed by a Mann–Whitney test to assess differences between groups. A threshold of $P < 0.05$ was defined as statistically significant.

Results

BBD-RSM-Based Enteric Coating Optimization and Pellet Preparation

The experimental runs with independent variables and the observed responses for the 17 formulations are shown in Table 2. Based on the Box-Behnken model, the factor combinations resulted in different drug release rates for EPs. The cumulative release rate within 6 h was very low (below 10%), indicating that the main limiting factor was the barrier action of the enteric coating. However, the cumulative release rate in PBS buffer (pH 7.6, 6–12 h) was much higher (more than 70%). To determine the levels of factors that yield optimum dissolution responses, mathematical relationships were generated between the dependent and independent variables using the experimental design software Design-Expert 8.0. The resulting equations in terms of coded factors for all the responses are given as follows:

$$Y_1 = 3.72 - 0.57X_1 - 0.20X_2 - 0.15X_3 + 0.075X_1X_2 - 0.025X_1X_3 + 0.075X_2X_3 - 0.22{X_1}^2 - 0.073{X_2}^2 - 0.22{X_3}^2 \left(R^2 = 0.9538\right) \quad (2)$$

Table 2 Experimental Runs and Observed Response Values for the Box-Behnken Design

Run	X_1	X_2	X_3	Cumulative Drug Release (%)		
				Y_1	Y_2	Y_3
1	2	10	20	2.5	6.5	70.38
2	1.25	15	20	3.2	8.1	73.27
3	1.25	10	15	3.9	13.9	77.69
4	2	5	15	2.9	7.8	72.50
5	1.25	10	15	3.6	12.7	76.84
6	0.5	10	10	4	17.1	82.28
7	2	15	15	2.7	9.5	73.78
8	1.25	15	10	3.2	14.6	75.05
9	2	10	10	3	11.7	72.33
10	1.25	5	10	3.8	16.8	80.66
11	1.25	10	15	3.9	14.3	76.84
12	1.25	10	15	3.6	12.9	75.56
13	0.5	10	20	3.6	10.2	78.54
14	1.25	5	20	3.5	9.7	77.01
15	0.5	15	15	3.8	11.8	79.22
16	1.25	10	15	3.6	13.5	76.24
17	0.5	5	15	4.3	16.2	81.68

$$Y_2 = 13.46 - 2.48X_1 - 0.81X_2 - 3.21X_3 + 1.52X_1X_2 + 0.43X_1X_3 + 0.15X_2X_3 - 1.53{X_1}^2 - 0.61{X_2}^2 - 0.55{X_3}^2 \left(R^2 = 0.9844\right) \quad (3)$$

$$Y_3 = 76.64 - 4.09X_1 - 1.32X_2 - 1.39X_3 + 0.93X_1X_2 + 0.45X_1X_3 + 0.47X_2X_3 - 0.23{X_1}^2 + 0.39{X_2}^2 - 0.52{X_3}^2 \left(R^2 = 0.9324\right) \quad (4)$$

Eqs. (2)–(4) represent the quantitative effect of the formulation independent variables X_1-X_3 on the three dependent responses Y_1-Y_3, respectively. The independent values of X_1-X_3 were ascertained in Eqs. (2)–(4) to obtain the predicted values of Y_1-Y_3. Furthermore, the relationship between the independent variables and dependent variables was illuminated and analysed using the three-dimensional (3D) response surface and two-dimensional (2D) contour plots shown in Figure 1.

As seen from Figure 1, when X_1, X_2 and X_3 increased, Y_1, Y_2 and Y_3 increased as well. It was found that the ratio of EUDRAGIT®FS 30D to EUDRAGIT®L 30D-55 (X_1), plasticizer concentration (X_2) and coating weight gain (X_3) were significant factors affecting Y_1, Y_2 and Y_3 (the cumulative drug release in 2 h, 6 h and 12 h). The model predicted Y_1, Y_2 and Y_3 values of 2.50, 6.34 and 70.92 when X_1, X_2 and X_3 were 2.0, 11.7 and 20.0, respectively. The results of three validation experiments showed that the predicted values and observed values were in reasonably close agreement (Table 3).[40]

Characterization of the β-CD Inclusion Complex

Figure 2A shows DSC curves of β-CD, volatile oil/β-CD physical mixture, volatile oil and the volatile oil/β-CD inclusion complex. The thermogram of β-CD showed a wide endothermic peak at approximately 145.48 °C, which referred to water release. There was another endothermic peak at approximately 314.24 °C, which was mainly related to the phase transition of β-CD. Volatile oil exhibited an endothermal effect peaking at approximately 307.40 °C, which was attributed to the decomposition of the volatile oil. The thermogram of the physical mixture was similar to the superimposition of the individual thermograms of β-CD and volatile oil. However, the thermogram of the inclusion complex exhibited a different pattern, and the two characteristic peaks of β-CD disappeared, indicating that water molecules in the cavity of β-CD were displaced.[41] Furthermore, a new characteristic peak

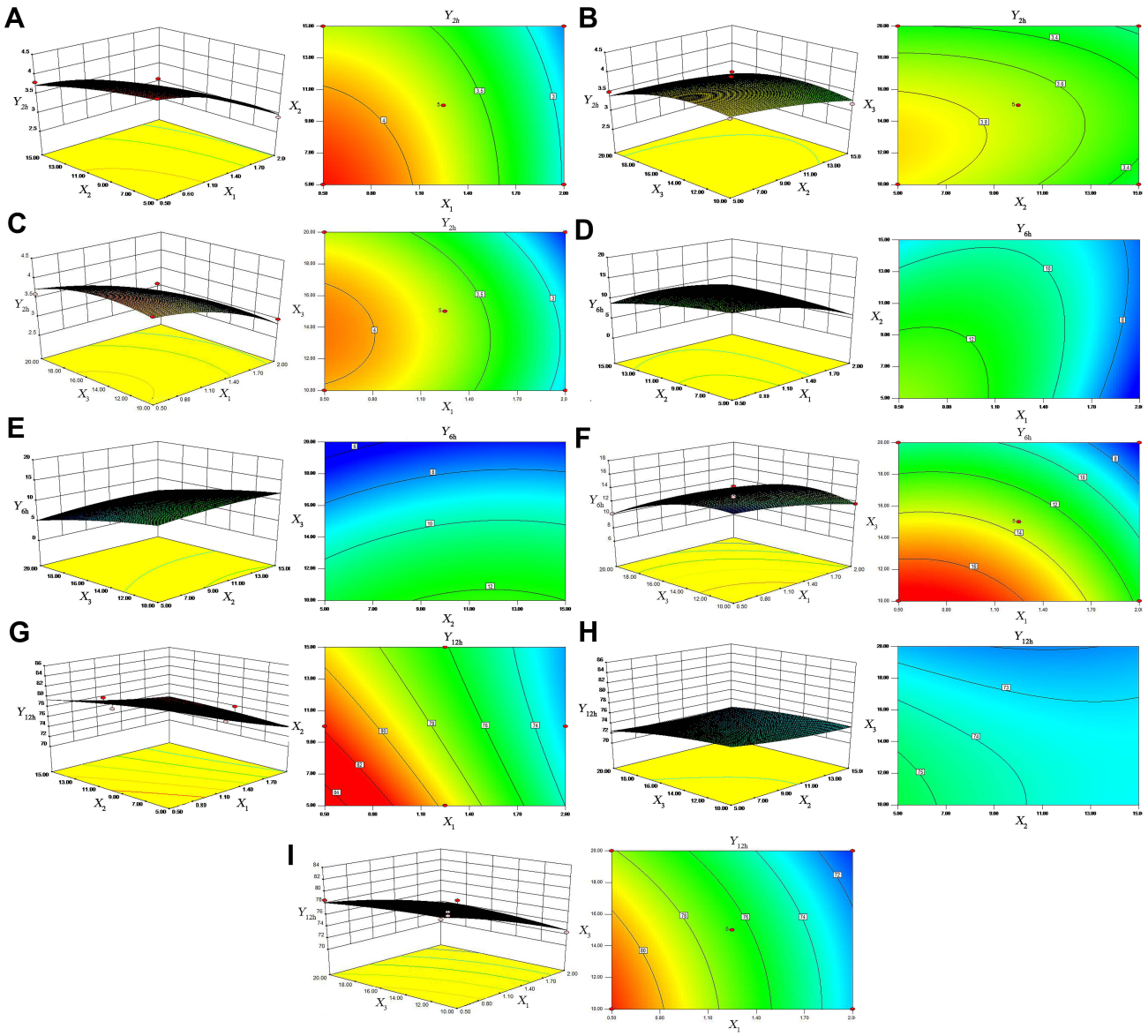

Figure 1 Effect of variables (X_1-X_3) on the response (Y_1-Y_3): 3D response surface plots and 2D contour plots. X_1: ratio of EUDRAGIT®FS 30D to EUDRAGIT®L 30D-55; X_2: plasticizer concentration (based on dry polymer weight); X_3: coating weight gain. Y_1-Y_3: cumulative drug release at 2 h, 6 h and 12 h. (**A**) the effects of X_1 and X_2 on Y_1; (**B**) the effects of X_2 and X_3 on Y_1; (**C**) the effects of X_1 and X_3 on Y_1; (**D**) the effects of X_1 and X_2 on Y_2; (**E**) the effects of X_2 and X_3 on Y_2; (**F**) the effects of X_1 and X_3 on Y_2; (**G**) the effects of X_1 and X_2 on Y_3; (**H**) the effects of X_2 and X_3 on Y_3; (**I**) the effects of X_1 and X_3 on Y_3.

appeared at 277.49 °C, which we speculated was due to the occurrence of an intermolecular interaction that generates a new phase rather than the volatile oil and β-CD. All these results indicate that the volatile oil was wrapped in the cavity of β-CD.

Table 3 Comparison Between the Observed and Predicted Responses of the Optimized Enteric Coating Layer

Evaluating Indexes	Observed	Predicted	Prediction Error (%)
Y_1	2.63	2.50	5.47%
Y_2	6.55	6.34	3.26%
Y_3	73.24	70.92	3.27%

X-ray powder diffraction can be used to determine the crystal type of crystal compounds. As shown in Figure 2B, β-CD exhibited many crystalline peaks between 5° and 50° (2θ =8.88, 12.47, 18.76 and 27.05°), indicating that β-CD mainly existed in a crystalline form. Volatile oil showed a large broad peak, suggesting that it is in an amorphous state. The XRD pattern of the physical mixture showed approximate superimposition of the individual patterns of β-CD and volatile oil. The inclusion complex exhibited different

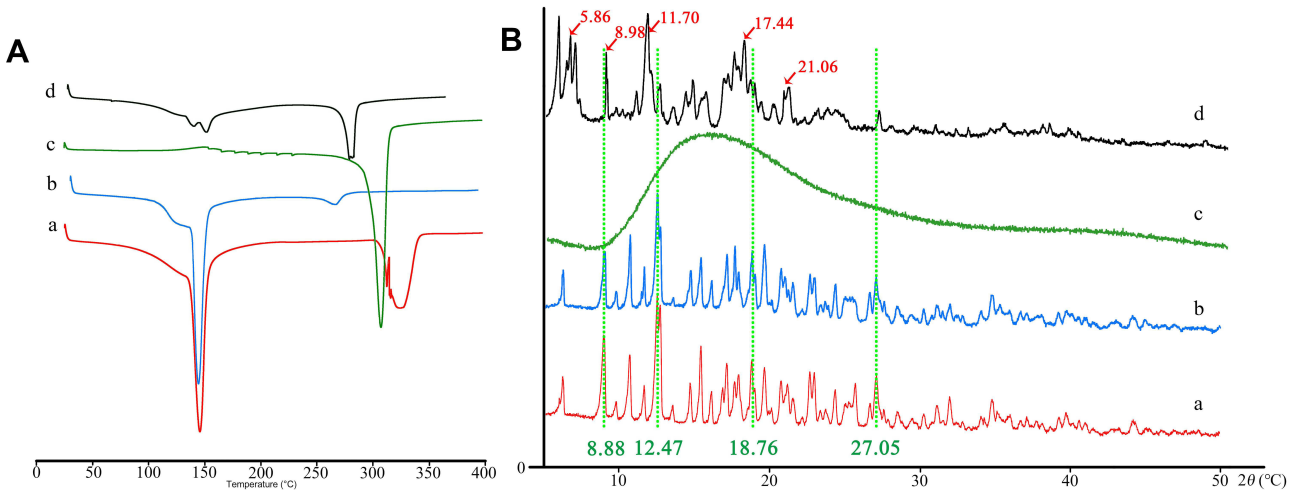

Figure 2 Characterization of the β-CD inclusion complex using DSC (**A**) and XRD (**B**): (a) β-CD; (b) volatile oil/β-CD physical mixture; (c) volatile oil; (d) volatile oil/β-CD inclusion complex.

main peaks (2θ =5.86, 8.98, 11.70, 17.44 and 21.06°) and distinctive peak patterns, with relatively broad bands compared with the physical mixture.[41] The appearance of these new characteristic peaks indicated that the inclusion complex was a new crystal form.

Characterization of Pellets

The WG (%), yield (%), RSD_w (%) and coating loss (%) for GPs, sub-Ps and EPs are listed in Table S2. The results showed that the preparation process employed for GPs, Sub-Ps and EPs was reasonable and repeatable and that the process stability was admirable.

According to the naked eye and SEM observations, the GPs were white and spherical or ellipsoid, while the EPs were yellow and brown spheres with smooth and round surfaces (Figure 3A and C (a and b)). Investigation of the morphology of these two pellets indicated that both GPs and EPs have a uniform size, ideal narrow size distribution, regular round shape and smooth surface.

The obtained particle size distribution of the coated pellets is presented in Table 4. The majority of the GPs and EPs lay within the intervals 700–830 μm (24–20 mesh) and 880–1180 μm (18–14 mesh). SEM images of

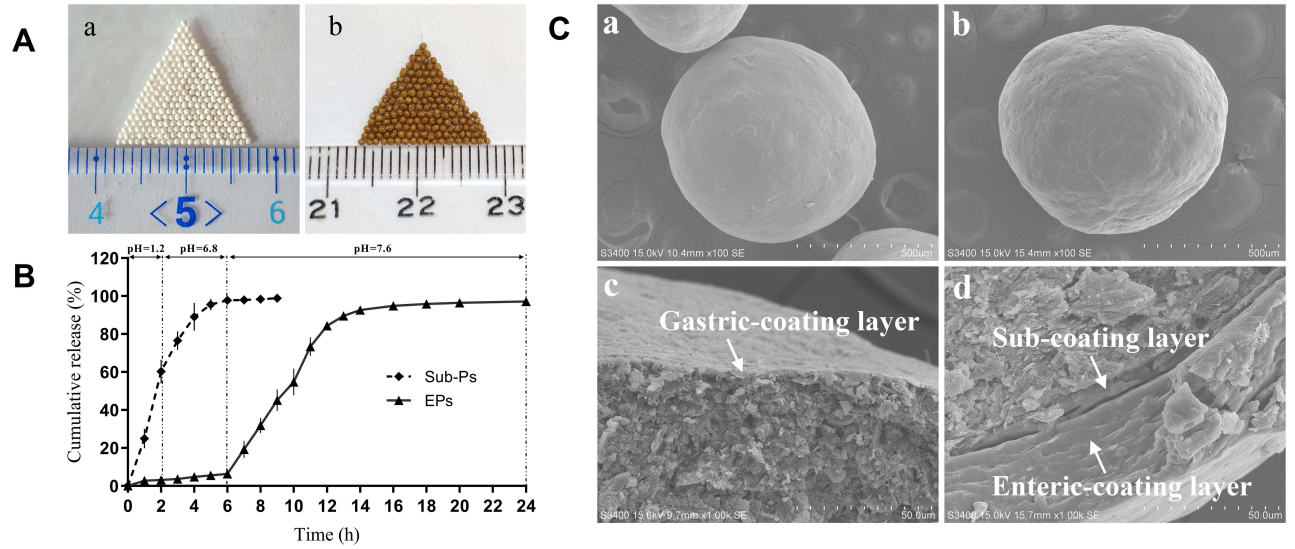

Figure 3 Physicochemical characterization of pellets. (**A**) Pellet size and shape observed by the naked eye. (a) GPs and (b) EPs (**B**) in vitro release profiles of Sub-Ps and EPs in different media (pH=1.2 for 2 h, pH=6.8 for 4 h, pH=7.6 for 18 h) (**C**) magnified scanning electron microscopy photograph of pellets. (a) Complete GPs and (b) complete EPs at 100×; (c) GPs cross-sections and (d) EPs cross-sections at 1000× in dissolution medium.

Table 4 The Particle Size Distribution of GPs and EPs (n=3)

GPs		EPs	
Size Distribution (Mesh)	**Mass Ratio (%)**	**Size Distribution (Mesh)**	**Mass Ratio (%)**
<30	5	<20	7
30–24	18	18–20	11
24–20	65	14–18	61
20–18	8	12–14	16
>18	4	>12	5

pellet cross-sections showing the structure of the inner region of the pellets are presented in Figure 3C (c). The sub coating layer (Figure 3C (d)) and polymer layer can be clearly observed in the cross-section views, indicating that the pellet core had a compact structure with the polymer layer tightly coated on the core.

Roundness, friability and bulk density are three important product quality requirements, and these parameters are presented in Table 5. The lower plane-critical angle and friability were related to the superior roundness and indicated that both GPs and EPs had good rigidity to avoid being smashed during the fluid-bed coating procedure.

HPLC-QQQ-MS and HPLC content determination methods were established for BBR and AT-1 to calculate drug loading and in vitro drug release. The good linearity of the determination method and the RSD of intraday/interday precision had a value smaller than 2% for each concentration level, which demonstrates good precision of the measurement. On this premise, the BBR and AT-1 loading in EPs and GPs was 125.61 ± 0.1 mg/g and 17.11 ± 0.16 mg/g, respectively.

The release profiles of the Sub-Ps and EPs are shown in Figure 3B. BBR release from the Sub-Ps without an enteric layer was immediate and almost complete within 4 h, demonstrating that Sub-Ps are not appropriate for colon drug delivery. Sufficient acid resistance was achieved when the Sub-Ps were coated with an enteric coating layer optimized by BBD-RSM. The cumulative release of BBR in artificial gastric medium (pH 1.2) for 2 h was less than 5% and that in artificial intestinal medium (pH 6.8) for 4 h was less than 10%. Exhilaratingly, almost 95% of BBR release occurred within 10 h thereafter in an artificial colonic medium (pH 7.6). The increase in the pH of the dissolution fluid (pH 7.6) significantly accelerates the rate of dissolution.

Table 5 Physical Characteristics of GPs and EPs (n=3, Mean ± SD)

Parameters	GPs	EPs
Roundness (θ/°)	12.17±0.35	9.73±1.50
Friability (*Fr*/%)	3.87±0.65	4.67±0.45
Bulk density (g/cm^3)	0.62±0.030	0.76±0.06

In vivo Imaging-Based Colon-Targeted Study of EPs

The results of the in vivo targeting evaluation of EPs are shown in Figure 4. Compared with coated pellets, the uncoated fluorescent pellets showed large dot-like fluorescence 1–2 h after oral administration, indicating that they began to disintegrate after reaching the stomach. At 4–6 h after oral administration, the entire small intestine treated with uncoated pellets was filled with fluorescence, indicating that most of the pellets had been disintegrated by this time. Eight to ten hours later, the fluorescence in the colon from the uncoated pellets gradually weakened due to their complete disintegration, and the fluorescein was quenched by the contents of the intestinal tract. However, the segment of the intestine from the ileocaecal region to the end of the colon was filled with fluorescence after oral administration of enteric coated fluorescent pellets, which means that a large number of pellets disintegrated and released the drug.

In vivo Pharmacokinetics Study

A pharmacokinetic study in SD rats after oral administration of DPs and BPC was performed, and the mean plasma concentration-time curve was constructed as shown in Figure 5. Lists of the corresponding pharmacokinetic parameters are shown in Table 6. As shown in Figure 5A, AT-1 can be quickly absorbed into the blood after oral administration of BPC and DPs. The T_{max} values of the two formulations were the same at 1.00 ± 0.00 h. The C_{max} values of BPC and DPs were 109.49 ± 5.61 ng/mL and 106.94 ± 11.43 ng/mL, respectively (P>0.05). These results indicate that inclusion of β-CD increases the solubility and dissolution of active ingredients in volatile oils. However, the T_{max} of AT-1 showed a "bimodal" phenomenon, indicating that there may be secondary absorption in the blood. Interestingly, the $AUC_{0\rightarrow t}$ value in the DPs group increased slightly compared with that in the BPC group, and the relative bioavailability value was 153.13%. Furthermore, the pattern showed a consistent plasma concentration of AT-1, indicating higher bioavailability in the DPs group. In addition, the DPs group had a higher MRT

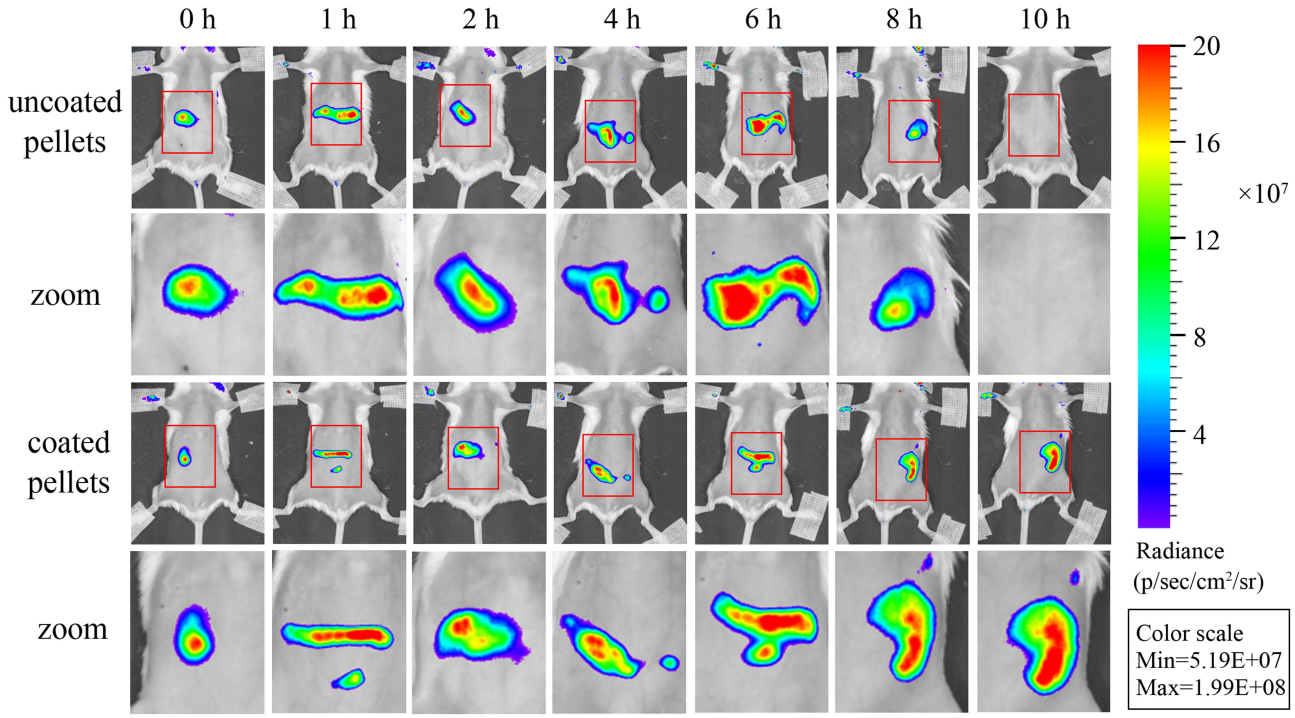

Figure 4 In vivo imaging of fluorescent colon-targeted pellets in mice.

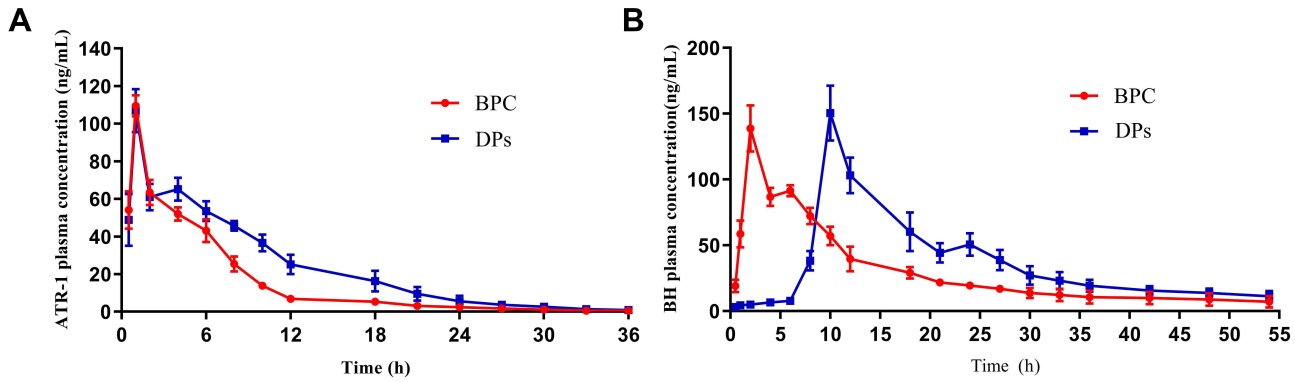

Figure 5 Pharmacokinetic profile of AT-1 (**A**) and BBR (**B**) in SD rats after oral administration of BPC and DPs at a single dose of 50 mg of AT-1 and 200 mg of BBR. Each value represents the mean ± SD (n = 3).

value than the BPC group, which means that AT-1 release from the pellets exhibited a certain sustained release effect.

According to Figure 5B, the T_{max} values of BBR in plasma from the BPC group and DPs group were 2.00 ± 0.00 and 10.00 ± 0.00 h, respectively. Furthermore, the obvious time lag in the DPs group indicated that the coated pellets had a good controlled release and a colon-specific effect. The T_{max} of both groups showed a "double peak" phenomenon due to enterohepatic circulation during BBR absorption.[42] The C_{max} of the DPs group was significantly different from that of the BPC group. The relative bioavailability in the two experimental groups was 121.38%, indicating a higher relative bioavailability of the DPs. In addition, the plasma drug concentration-time curve was gentler, and the DPs group had a higher MRT value than the BPC group, indicating an obvious sustained release effect in the DPs group, which can better stabilize the blood drug concentration and thus increase bioavailability.

Anti-Ulcerative Colitis Analysis

Effect of UC on Body Weight

Figure 6 shows that the body weight of rats in healthy control group A slightly increased over time. All the DSS-

Table 6 Pharmacokinetic Parameters of AT-1 and BBR Delivered by DPs and BPC After Oral Administration (n=3, Mean ± SD)

Parameters	AT-1		BBR	
	BPC	DPs	BPC	DPs
C_{max} (ng/mL)	109.49±5.61	106.94±11.43	138.81±17.63	150.43±20.82
T_{max} (h)	1.00±0.00	1.00±0.00	2.00±0.00	10.00±0.00
$AUC_{0\rightarrow t}$ (ng·h/mL)	543.91±50.24	832.87±130.73	1588.79±160.65	1928.56±297.47
$AUC_{0\rightarrow\infty}$(ng·h/mL)	547.34±51.74	839.04±134.06	1888.77±524.25	2393.53±418.88
$T_{1/2}$ (h)	4.94±1.06	4.1±1.54	22.82±16.57	26.74±13.97
MRT (h)	6.38±0.66	8.75±0.91	26.36±16.91	36.05±12.29
F_{rel} (%)	-	153.13	-	121.38

Abbreviations: UC, ulcerative colitis; BBR, Berberine; CC, *Coptis chinensis* Franch; AM, *Atractylodes macrocephala* Koidz; DPs, dual-targeted pellets; OCDDS, oral colon-targeted drug delivery system; DSS, dextran sulfate sodium salt; AT-1, Atractylenolide I; β-CD, β-cyclodextrin; MCC, Microcrystalline cellulose; HPMC, Hypromellose; SASP, Sulfasalazine; BBD-RSM, Box Behnken design of a response surface methodology; GPs, Gastric coated pellets; Eps, Enteric coated pellets; Sub-Ps, EPs core coated with 4% HPMC as sub-coating layer; BPC, bulk pharmaceutical chemicals.

induced groups showed the lowest body weight on day 7 or day 8, and the haematochezia and diarrhoea symptoms were most severe on these two days in the experimental process, which indicated that the establishment of the UC model was successful. After day 8, the body weight of rats in almost all the DSS-induced groups showed an upward trend, indicating that each drug administration group had a certain effect on alleviating the weight loss caused by UC. Among them, the DPs medium-dose group G and SASP group C showed the most effectiveness.

Effect of DPs Administration on the Clinical Activity Score in DSS-Induced UC

As shown in Figure 7, for all the DSS-induced groups, the DAI score increased rapidly and consistently over the 6 days of the induction experiment. Starting on day 7, all drug-receiving groups showed a decrease in inflammation severity after a lag time of 24 to 48 h and a reduction in the DAI score. The maximum reduction was observed in the DPs medium- and high-dose groups on day 14. This reflects the efficacy of the prepared DPs, and a dose of 50 mg/kg AT-1 + 100 mg/kg BBR in rats was inferred to be sufficient to achieve satisfactory therapeutic efficacy. In the case of group F, the DAI index was observed to be significantly lower than that of model group B on day 14 (Figure 8A), indicating a partial reversal of inflammation even at a dose of 50 mg/kg AT-1 + 50 mg/kg BBR. In addition, the DAI score of groups G and H was also found to be significantly lower ($P<0.05$) than that of SASP group C, indicating better efficacy of DPs against inflammation induced by UC. Nevertheless, in both groups A and B,

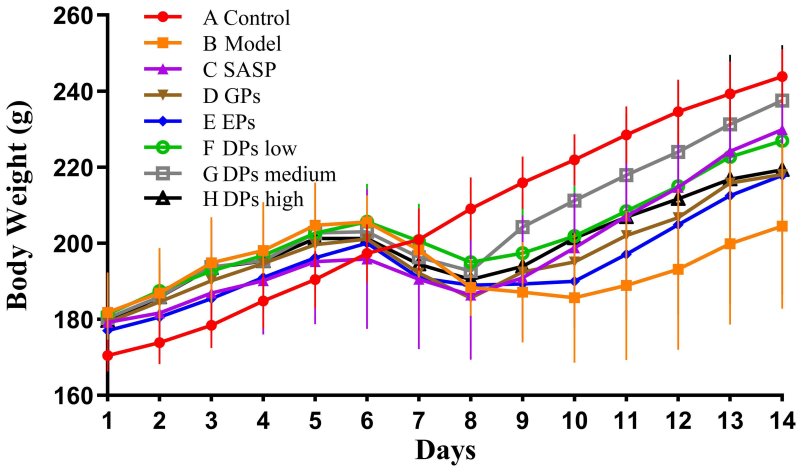

Figure 6 Time-dependent variations in body weight. (**A**) Control group, (**B**) model group, (**C**) SASP group, (**D**) GPs group, (**E**) EPs group, (**F**) DPs low-dose group, (**G**) DPs medium-dose group, (**H**) DPs high-dose group (n = 10).

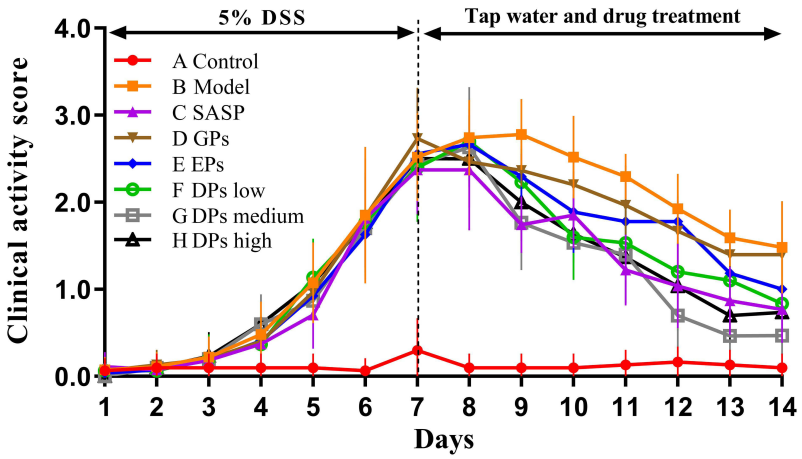

Figure 7 Clinical activity scores (DAI) throughout the entire experimental period. (**A**) Control group, (**B**) model group, (**C**) SASP group, (**D**) GPs group, (**E**) EPs group, (**F**) DPs low-dose group, (**G**) DPs medium-dose group, (**H**) DPs high-dose group (n = 10).

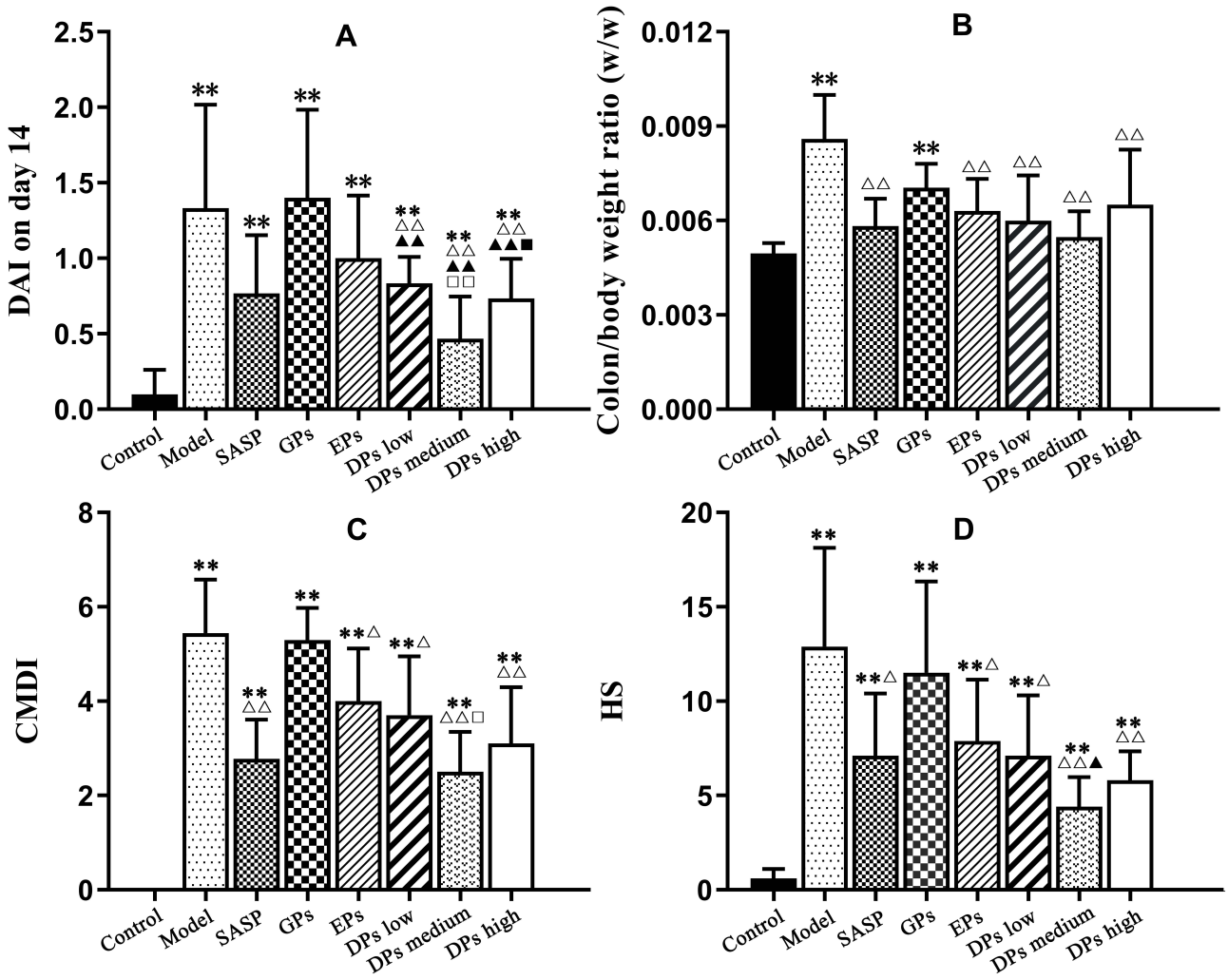

Figure 8 (**A**) Scoring of disease activity index (DAI) in each group, (**B**) The colon/body weight ratio, (**C**) scoring of colon mucosal damage index (CMDI) and (**D**) microscopic histological changes on day 14 ($\bar{x} \pm s$, n=10). Comparisons: **P<0.01 vs control group, $^{\triangle}P$<0.05, $^{\triangle\triangle}P$<0.01 vs model group, $^{\blacktriangle}P$<0.05, $^{\blacktriangle\blacktriangle}P$<0.01 vs SASP group, $^{\square}P$<0.05, $^{\square\square}P$<0.01 vs DPs low-dose group, $^{\blacksquare}P$<0.05 vs DPs medium-dose group, **P<0.01 vs control group.

https://doi.org/10.2147/DDDT.S322702 DovePress

the treatment was less effective in reducing the DAI score. This gives a clear indication that the DPs exhibited enhanced efficacy compared with GPs or EPs monotherapy, which resulted in a markedly reduced DAI score.

Effect of DPs Administration on the Colon/Body Weight Ratio and Macroscopic Injury Score

As shown in Figure 8B, GPs administration did not exert a significant effect; however, in the other drug administration groups, the C/B ratio was significantly reduced.

The colon mucosal damage index (CMDI) is shown in Figure 8C. The results showed that the colorectal morphology in the rats in the control group was normal, and the inner wall of the intestine was smooth and elastic. The colour of the intestinal wall in all the DSS-induced groups was dark red. Diffuse oedema and destruction of the mucous membranes appeared in all parts of the intestinal wall. The CMDI scores of the rats in each administration group were significantly different from those in the control group ($P<0.01$). Except for the EPs group, there were significant differences between each administration group and the model group ($P<0.05$), indicating that each treatment administered had a certain effect in improving colorectal mucosal damage. The DPs medium-dose group had a lower score than the other administration groups, indicating that a better therapeutic effect was observed in the DPs medium-dose group.

Effect of DPs Administration on Microscopic Colon Damage in DSS-Induced UC

H&E-stained colon tissue sections (Figure 9) show that rats in the control group had basically no abnormalities. Colonic epithelial cells were intact, crypts were arranged in order, and goblet cells were adequate, with no signs of inflammation or tissue morphological damage. However, in the other groups, obvious inflammatory cell infiltration was present in the colon. The mucosal epithelial cells fell off to varying degrees, goblet cells were decreased, and crypts were arranged disorderly. The model group showed a large area of deep inflammatory cell infiltration, glandular deformation and goblet cell loss. The colon tissue mucosal epithelial lesions of the rats in each administration group were reduced to a different extent than those of the rats in the model group. Some small ulcers were still present, but the histopathological score (Figure 8D) for the colon was lower than that for the model group. The inflammation and lesions of the colon tissue in the DPs medium- and high-dose groups were significantly reduced. The crypts and glands were arranged in an orderly manner, indicating superior anti-inflammatory effects.

Effect of DPs Administration on Inflammatory Factors and Immunoglobulins

As shown in Figure 10, the expression level of IL-1β in the serum and tissues of rats in the DPs high-dose group was not significantly different from that in the control group, indicating that the rats had basically recovered under

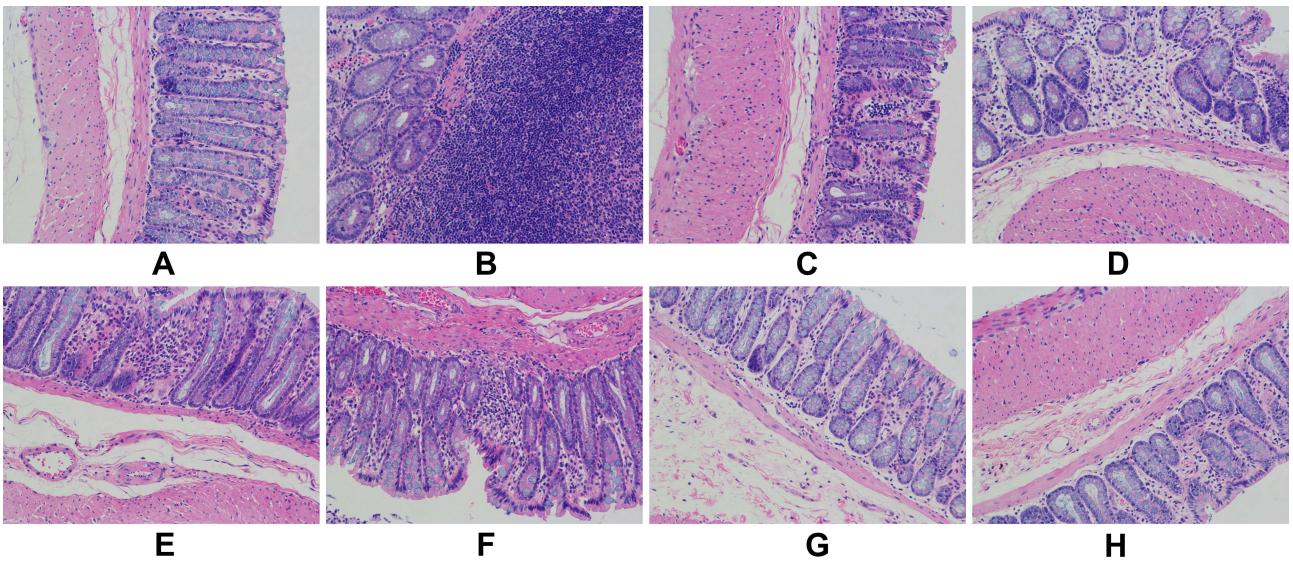

Figure 9 Pathological colon sections stained with H&E in each group (200 ×) (**A**) control group, (**B**) model group, (**C**) SASP group, (**D**) GPs group, (**E**) EPs group, (**F**) DPs low dose-group, (**G**) DPs medium-dose group, (**H**) DPs high-dose group.

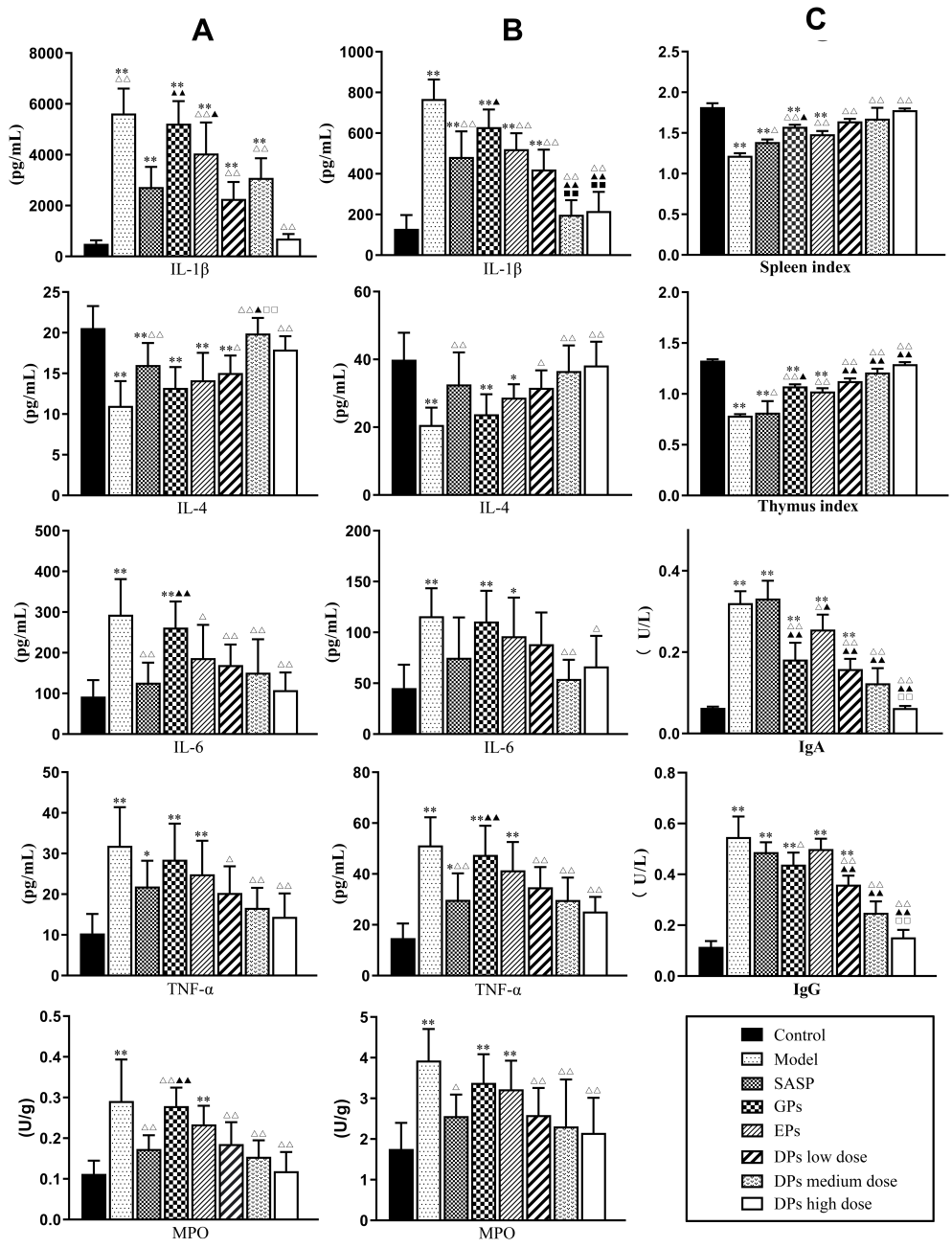

Figure 10 The effects of each treatment on the expression of inflammatory factors and immune-related indicators ($\bar{x} \pm s$, n=10). (**A**) Serum, (**B**) colon tissue, (**C**) serum. Comparisons: **P*<0.05, ***P*<0.01 vs control group, $^{\triangle}$*P*<0.05, $^{\triangle\triangle}$*P*<0.01 vs model group, $^{\blacktriangle}$*P*<0.05, $^{\blacktriangle\blacktriangle}$*P*<0.01 vs SASP group, $^{\square\square}$*P*<0.01 vs DPs low-dose group, $^{\blacksquare\blacksquare}$*P*<0.05 vs DPs medium-dose group.

treatment with high-dose DPs. In the serum, except for the GPs group, each administration group showed a significant difference compared with the model group ($P<0.01$), indicating that the effect of drug intervention was better than the effect of autologous recovery. The treatment with DPs in the medium/high-dose groups had significant effects on increasing the expression of IL-4 in serum and tissues ($P<0.01$), and the promotive effect of IL-4 expression in the medium-dose group was more obvious. The control group was only had significantly different from the model group, the EPs group and GPs groups ($P<0.05$), while the expression of IL-6 was clearly inhibited in the other groups. The expression level of IL-6 was more significantly decreased in the DPs medium/high-dose groups ($P<0.01$). In addition, the expression level of TNF-α in the DPs groups was not significantly different from that in the control group ($P>0.05$) in either serum or tissue, indicating that the DPs had a great effect on inhibiting the

expression of TNF-α. Additionally, there was a significant difference between the DPs medium dose, DPs high dose, SASP and model groups ($P<0.01$), indicating that the activity of MPO was effectively inhibited in all three groups. All the results showed that DPs have great anti-inflammatory effects, and the activity was even better than that of the positive control drug SASP and administration of EPs alone.

Compared with the control group, the spleen index and thymus index of the model rats were decreased, and the IgA and IgG levels in the serum were increased. Compared with the model group, the spleen index and thymus index of the rats in each DPs dose group were increased in a dose-dependent manner, and the IgA and IgG levels in the serum were also decreased in a dose-dependent manner.

In the present study, after treatment with AM volatile oil-loaded GPs, the expression levels of IgA and IgG were obviously decreased. However, the levels were still significantly different from those in the healthy control group. To our satisfaction, the IgA and IgG concentrations in the DPs groups were decreased significantly. In particular, there was no significant difference between the DPs medium/high-dose groups and the control group ($P>0.05$), suggesting that DPs can improve the immune function of rats with UC.

Discussion

Ulcerative colitis (UC) is a common autoimmune disease and is difficult to heal, or even lead to colon cancer in severe cases. At present, the clinical treatment of UC is still dominated by drug methods, while the commonly used chemotherapeutic drugs have some disadvantages that can only alleviate symptoms, and it is difficult to cure and the adverse reactions are obvious, which reduces the patient's compliance. Traditional Chinese medicine has unique advantages in the treatment of chronic gastrointestinal diseases caused by multiple reasons. It also pays attention to the overall balance while symptomatic treatment. In this study, two traditional Chinese medicines BBR and AM volatile oil were combined with an oral colon-specific drug delivery system, and the research was carried out on the preparation and in vitro-in vivo evaluation of DPs. Our results demonstrated that oral administration of DPs could effectively relieve the symptoms in UC rats' model, and the anti-UC mechanism may be related not only to inhibiting inflammation but also to enhancing body immunity.

In recent decades, state of the art small-animal imaging modalities provide non-invasive images rich in quantitative anatomical and functional information, which renders longitudinal studies possible allowing precise monitoring of disease progression and response to therapy in models of different diseases.[43] Our research is significant because it offers the possibility of using in vivo imaging to position the delivery of oral preparation. Photographs were taken at regular intervals to observe transport and drug release from the pellets in the gastrointestinal tract. According to our vision, if the coating of the pellet is not destroyed, it should emit dot-like or flaky-like fluorescence. After the coating was dissolved, the punctate fluorescence gradually spread throughout the gastrointestinal tract with the release of the drug. Combined with the fluorescence signal and the anatomical features of the gastrointestinal tract of mice, the transport position of the EPs in the gastrointestinal tract can be judged to evaluate their in vivo targeting characteristics. To our satisfaction, in vivo targeting evaluation results showed that the EPs have good colon targeting properties and can be transported to the colon to release drugs after oral administration, thereby promoting drug absorption and improving drug efficacy.

MPO is an index of neutrophil recruitment in the murine UC model. Therefore, the MPO activity may reflect more specific inflammatory events compared with cytokine concentrations. In our study, the colonic MPO activity was significantly increased in the DSS group compared with the normal control group, and the group received with DPs showed significantly ($P < 0.01$) decreased MPO activity (Figure 10). Accordingly, DPs blocks neutrophil infiltration into injured tissues. Cytokines are considered crucial signals in the intestinal immune system, and immune cells, such as, T cells, dendritic cells, macrophages, and intestinal epithelial cells, are involved in the secretion of various cytokines that regulate the inflammatory response in UC. Previous studies have revealed elevated levels of cytokines, such as TNF-α, IFN-γ, IL-1β, IL-6, IL-17, and IL- 21, in UC.[30,44,45] In our study, we detected increased expression levels of TNF-α, IL-1β and IL-6 in DSS-induced mice. However, the oral administration of DPs resulted in decreased expression levels of the above-mentioned proinflammatory cytokine.

The spleen and thymus are important immune organs in the body. It has been reported that the spleen index and thymus index of rats with UC are significantly reduced, and the immune capacity of organs is reduced.[46] Immunoglobulins participate in humoral immunity, and

the increased levels of IgA and IgG suggest that the humoral immunity of rats with UC is hyperactive, which may be a compensatory effect in response to the reduced cellular immunity. Studies have shown that an imbalance in the secretion of anti-inflammatory and pro-inflammatory factors is an important link in the intestinal inflammatory lesions of patients with UC. An increase in the levels of pro-inflammatory factors is involved in cellular immunity and promotes intestinal inflammatory responses, which can cause further damage to intestinal tissues. In our research, the expression levels of pro-inflammatory factors include TNF-α, IL-1β and IL-6 in DPs received rats' groups were significantly decreased, and the expression level of anti-inflammatory factors such as IL-4 was relatively increased. In addition, the IgA and IgG concentrations in the DPs groups were significantly decreased. In summary, the orally deliverable DPs have a synergistic treatment effects for UC. It can regulate body immunity while exerting anti-inflammatory effects. The research of this subject is expected to provide a new drug for the treatment of UC.

Conclusions

A promising dual-targeted pellet loaded with BBR and AM volatile oil was developed for the treatment of UC. BBR was loaded in the enteric soluble layer for colon-targeted release and thus had a local effect. AM volatile oil loaded in stomach-targeted pellets was prepared by extrusion-spheronization and fluid bed techniques, with HPMC as the gastric soluble layer, resulting in quick release and a systemic effect. The optimized EPs and GPs both have satisfying physicochemical characteristics. The bioavailability of BBR and AT-1 was much higher after pelletizing. The in vivo targeting evaluation showed that EPs have great acid resistance and satisfactory colon-targeting ability. The GPs disintegrated in 5 min in the stomach, allowing complete drug release. The synergistic effect of DPs ameliorated the clinical symptoms of UC, inhibited the expression of several inflammatory cytokines and decreased the levels of IgA and IgG. This suggests that the anti-UC mechanism may be related not only to inhibiting inflammation but also to enhancing body immunity. Thus, the developed oral dual-targeted delivery system could substantially contribute to the management of UC and might provide a pharmaceutical strategy for the synergistic treatment of gastrointestinal tract diseases.

Acknowledgments

The work was supported by the projects of the National Natural Science Foundation of China (81873011, 82074272), the Science and Technology Commission of Shanghai Municipality (20S21900300, 21XD1403400), the Outstanding Talents Program of Shanghai Health and Family Planning Commission (2018BR27). The authors thank the professor Fuzheng Ren of Shanghai Key Laboratory of New Drug Design, School of Pharmacy, East China University of Science and Technology, Shanghai, China, for his help in using the extruded-spheronizing granulator and fluidized bed coating-machine for this study.

Disclosure

The authors declare no conflicts of interest in this work.

References

1. Abraham C, Cho JH. Inflammatory bowel disease. *N Engl J Med*. 2009;361(21):2066–2078. doi:10.1056/NEJMra0804647
2. Sicilia B, Garcia-Lopez S, Gonzalez-Lama Y, Zabana Y, Hinojosa J, Gomollon F. GETECCU 2020 guidelines for the treatment of ulcerative colitis developed using the GRADE approach. *Gastroenterol Hepatol*. 2020;43(Suppl 1):1–57. doi:10.1016/j.gastrohep.2020.07.001
3. Gajendran M, Loganathan P, Jimenez G, et al. A comprehensive review and update on ulcerative colitis(). *Dis Mon*. 2019;65(12):100851. doi:10.1016/j.disamonth.2019.02.004
4. Han W, Xie B, Li Y, Shi L, Wang H. Orally deliverable nanotherapeutics for the synergistic treatment of colitis-associated colorectal cancer. *Theranostics*. 2019;9(24):7458–7473. doi:10.7150/thno.38081
5. Grivennikov SI. Inflammation and colorectal cancer: colitis-associated neoplasia. *Semin Immunopathol*. 2013;35:229–244.
6. Danese S, Mantovani A. Inflammatory bowel disease and intestinal cancer: a paradigm of the Yin-Yang interplay between inflammation and cancer. *Oncogene*. 2010;29(23):3313–3323. doi:10.1038/onc.2010.109
7. Porter RJ, Kalla R, Ho GT. Ulcerative colitis: recent advances in the understanding of disease pathogenesis. *F1000Res*. 2020;9:294. doi:10.12688/f1000research.20805.1
8. Wang R, Zhou G, Wang M, Peng Y, Li X. The metabolism of polysaccharide from Atractylodes macrocephala Koidz and its effect on intestinal microflora. *Evid Based Compl Alt*. 2014;2014:1–7.
9. Zhang L, Cao N, Wang Y, et al. Improvement of oxazolone-induced ulcerative colitis in rats using andrographolide. *Molecules*. 2020;25(1):76. doi:10.3390/molecules25010076
10. Kringel DH, Antunes MD, Klein B, et al. Production, characterization, and stability of orange or eucalyptus essential oil/beta-cyclodextrin inclusion complex. *J Food Sci*. 2017;82(11):2598–2605. doi:10.1111/1750-3841.13923
11. Tan S, Yu W, Lin Z, et al. Berberine ameliorates intestinal mucosal barrier damage induced by peritoneal air exposure. *Biol Pharm Bull*. 2015;38(1):122–126. doi:10.1248/bpb.b14-00643
12. Li YH, Xiao H, Hu D, et al. Berberine ameliorates chronic relapsing dextran sulfate sodium-induced colitis in C57BL/6 mice by suppressing Th17 responses. *Pharmacol Res*. 2016;110:S1943242085.
13. Liao Z, Xie Y, Zhou B, et al. Berberine ameliorates colonic damage accompanied with the modulation of dysfunctional bacteria and functions in ulcerative colitis rats. *Appl Microbiol Biotechnol*. 2020;104(4):1737–1749. doi:10.1007/s00253-019-10307-1

14. Leopold CS, Eikeler D. Basic coating polymers for the colon-specific drug delivery in inflammatory bowel disease. *Drug Dev Ind Pharm*. 2000;26(12):1239–1246. doi:10.1081/DDC-100102305
15. Yang L, Chu JS, Fix JA. Colon-specific drug delivery: new approaches and in vitro/in vivo evaluation. *Int J Pharmaceut*. 2002;235(1):1–15. doi:10.1016/S0378-5173(02)00004-2
16. Lee SH, Bajracharya R, Min JY, Han JW, Park BJ, Han HK. Strategic approaches for colon targeted drug delivery: an overview of recent advancements. *Pharmaceutics*. 2020;12(1):68.
17. Wang Q, Wang G, Zhou J, Gao L, Cui Y. Colon targeted oral drug delivery system based on alginate-chitosan microspheres loaded with icariin in the treatment of ulcerative colitis. *Int J Pharmaceut*. 2016;515(1–2):176–185. doi:10.1016/j.ijpharm.2016.10.002
18. Xiao B, Merlin D. Oral colon-specific therapeutic approaches toward treatment of inflammatory bowel disease. *Expert Opin Drug Del*. 2012;9(11):1393–1407. doi:10.1517/17425247.2012.730517
19. Pandey S, Swamy S, Gupta A, et al. Multiple response optimisation of processing and formulation parameters of pH sensitive sustained release pellets of capecitabine for targeting colon. *J Microencapsul*. 2018;35(3):259–271. doi:10.1080/02652048.2018.1465138
20. Sun X, Liu C, Omer AM, et al. pH-sensitive ZnO/carboxymethyl cellulose/chitosan bio-nanocomposite beads for colon-specific release of 5-fluorouracil. *Int J Biol Macromol*. 2019;128:468–479. doi:10.1016/j.ijbiomac.2019.01.140
21. Moghimipour E, Rezaei M, Kouchak M, et al. Effects of coating layer and release medium on release profile from coated capsules with Eudragit FS 30D: an in vitro and in vivo study. *Drug Dev Ind Pharm*. 2018;44(5):861–867. doi:10.1080/03639045.2017.1415927
22. Wan D, Zhao M, Zhang J, Luan L. Development and in vitro-in vivo evaluation of a novel sustained-release loxoprofen pellet with double coating layer. *Pharmaceutics*. 2019;11(6):260. doi:10.3390/pharmaceutics11060260
23. Segale L, Mannina P, Giovannelli L, Muschert S, Pattarino F. Formulation and coating of alginate and alginate-hydroxypropylcellulose pellets containing ranolazine. *J Pharm Sci US*. 2016;105(11):3351–3358. doi:10.1016/j.xphs.2016.08.001
24. Kim Y, Pradhan R, Paudel BK, Choi JY, Im HT, Kim JO. Preparation and evaluation of enteric-coated delayed-release pellets of duloxetine hydrochloride using a fluidized bed coater. *Arch Pharm Res*. 2015;38(12):2163–2171. doi:10.1007/s12272-015-0590-y
25. Melegari C, Bertoni S, Genovesi A, et al. Ethylcellulose film coating of guaifenesin-loaded pellets: a comprehensive evaluation of the manufacturing process to prevent drug migration. *Eur J Pharm Biopharm*. 2016;100:15–26. doi:10.1016/j.ejpb.2015.12.001
26. Belew S, Suleman S, Duguma M, et al. Development of a dissolution method for lumefantrine and artemether in immediate release fixed dose artemether/lumefantrine tablets. *Malar J*. 2020;19(1):139. doi:10.1186/s12936-020-03209-5
27. Verstraete G, De Jaeghere W, Vercruysse J, et al. The use of partially hydrolysed polyvinyl alcohol for the production of high drug-loaded sustained release pellets via extrusion-spheronisation and coating: in vitro and in vivo evaluation. *Int J Pharmaceut*. 2017;517(1–2):88–95. doi:10.1016/j.ijpharm.2016.11.067
28. Novobilsky A, Hoglund J. Small animal in vivo imaging of parasitic infections: a systematic review. *Exp Parasitol*. 2020;214:107905. doi:10.1016/j.exppara.2020.107905
29. Karrout Y, Dubuquoy L, Piveteau C, et al. In vivo efficacy of microbiota-sensitive coatings for colon targeting: a promising tool for IBD therapy. *J Control Release*. 2015;197:121–130. doi:10.1016/j.jconrel.2014.11.006
30. Pandurangan AK, Ismail S, Saadatdoust Z, Esa NM. Allicin alleviates dextran sodium sulfate- (DSS-) induced ulcerative colitis in BALB/c mice. *Oxid Med Cell Longev*. 2015;2015:605208. doi:10.1155/2015/605208
31. Ferri D, Costero AM, Gavina P, et al. Efficacy of budesonide-loaded mesoporous silica microparticles capped with a bulky azo derivative in rats with TNBS-induced colitis. *Int J Pharm*. 2019;561:93–101. doi:10.1016/j.ijpharm.2019.02.030
32. Shi C, Liang Y, Yang J, et al. MicroRNA-21 knockout improve the survival rate in DSS induced fatal colitis through protecting against inflammation and tissue injury. *Plos One*. 2013;8(6):e66814. doi:10.1371/journal.pone.0066814
33. Nunes NS, Chandran P, Sundby M, et al. Therapeutic ultrasound attenuates DSS-induced colitis through the cholinergic anti-inflammatory pathway. *Ebiomedicine*. 2019;45:495–510. doi:10.1016/j.ebiom.2019.06.033
34. Li X, Xu Y, Zhang C, et al. Protective Effect of Calculus Bovis Sativus on Dextran Sulphate Sodium-Induced Ulcerative Colitis in Mice. *Evid-Based Compl Alt*. 2015;2015:Article ID 469506. doi:10.1155/2015/469506
35. Gao W, Wang C, Yu L, et al. Chlorogenic Acid Attenuates Dextran Sodium Sulfate-Induced Ulcerative Colitis in Mice through MAPK/ERK/JNK Pathway. *Biomed Res Int*. 2019;2019:Article ID: 6769789. doi:10.1155/2019/6769789
36. Ke J, Bian X, Liu H, et al. Edaravone reduces oxidative stress and intestinal cell apoptosis after burn through up-regulating miR-320 expression. *Mol Med*. 2019;25:54. doi:10.1186/s10020-019-0122-1
37. Kverka M, Rossmann P, Tlaskalova-Hogenova H, et al. Safety and efficacy of the immunosuppressive agent 6-tioguanine in murine model of acute and chronic colitis. *Bmc Gastroenterol*. 2011;11(1):47. doi:10.1186/1471-230X-11-47
38. Banerjee A, Bizzaro D, Burra P, et al. Umbilical cord mesenchymal stem cells modulate dextran sulfate sodium induced acute colitis in immunodeficient mice. *Stem Cell Res Ther*. 2015;6:79. doi:10.1186/s13287-015-0073-6
39. Neurath MF. Cytokines in inflammatory bowel disease. *Nat Rev Immunol*. 2014;14(5):329–342. doi:10.1038/nri3661
40. Kramar A, Turk S, Vrečer F. Statistical optimisation of diclofenac sustained release pellets coated with polymethacrylic films. *Int J Pharmaceut*. 2003;256(1–2):43–52. doi:10.1016/S0378-5173(03)00061-9
41. Wang X, Luo Z, Xiao Z. Preparation, characterization, and thermal stability of β-cyclodextrin/soybean lecithin inclusion complex. *Carbohyd Polym*. 2014;101:1027–1032. doi:10.1016/j.carbpol.2013.10.042
42. Kumar A, Ekavali CK, Mukherjee M, Pottabathini R, Dhull DK, Dhull DK. Current knowledge and pharmacological profile of berberine: an update. *Eur J Pharmacol*. 2015;761:288–297. doi:10.1016/j.ejphar.2015.05.068
43. Lauber DT, Fulop A, Kovacs T, Szigeti K, Mathe D, Szijarto A. State of the art in vivo imaging techniques for laboratory animals. *Lab Anim*. 2017;51(5):465–478. doi:10.1177/0023677217695852
44. Araki A, Nara H, Rahman M, et al. Role of interleukin-21 isoform in dextran sulfate sodium (DSS)-induced colitis. *Cytokine*. 2013;62(2):262–271. doi:10.1016/j.cyto.2013.03.006
45. Pervin M, Hasnat MA, Lim JH, et al. Preventive and therapeutic effects of blueberry (Vaccinium corymbosum) extract against DSS-induced ulcerative colitis by regulation of antioxidant and inflammatory mediators. *J Nutr Biochem*. 2016;28:103–113. doi:10.1016/j.jnutbio.2015.10.006
46. Gong Y, Niu W, Tang Y, et al. Aggravated mucosal and immune damage in a mouse model of ulcerative colitis with stress. *Exp Ther Med*. 2019;17(3):2341–2348.